Spin separation in a T ballistic nanojunction due to lateral-confinement-induced spin–orbit coupling

2007 J. Phys.: Condens. Matter 19 395018

(http://iopscience.iop.org/0953-8984/19/39/395018)

IOP PUBLISHING JOURNAL OF PHYSICS: CONDENSED MATTER

J. Phys.: Condens. Matter **19** (2007) 395018 (9pp) doi:10.1088/0953-8984/19/39/395018

Spin separation in a T ballistic nanojunction due to lateral-confinement-induced spin–orbit coupling

S Bellucci[1], F Carillo[2] and P Onorato[1,3]

[1] INFN, Laboratori Nazionali di Frascati, PO Box 13, 00044 Frascati, Italy
[2] NEST-INFM-CNR and Scuola Normale Superiore, I-56126 Pisa, Italy
[3] Department of Physics 'A Volta', University of Pavia, Via Bassi 6, I-27100 Pavia, Italy

Received 22 February 2007, in final form 13 May 2007
Published 30 August 2007
Online at stacks.iop.org/JPhysCM/19/395018

Abstract

We propose a new scheme of spin filtering employing ballistic nanostructures in two-dimensional electron gases (2DEGs). The proposal is essentially based on the spin–orbit (SO) interaction arising from the lateral confining electric field. This sets the basic difference from other works employing ballistic crosses and T junctions with the conventional SO term arising from 2DEG confinement. We discuss the consequences of this different approach for the magnetotransport properties of the device, showing that the filter can in principle be used not only to generate a spin polarized current but also to perform an electric measurement of the spin polarization of a charge current. We focus on single-channel transport and investigate numerically the spin polarization of the current.

(Some figures in this article are in colour only in the electronic version)

1. Introduction

In recent years much effort has been devoted to the study and the realization of electric field controlled spin based devices [1]. Many basic building blocks are today investigated theoretically and experimentally in order to realize a fully spin based circuitry. Of particular relevance are: (i) pure spin current generation, (ii) voltage control of the spin polarization of a current and (iii) the electric detection of this polarization. For the same purpose many works have been focusing on the so-called spin Hall effect [2–7] and most of the implementations in two-dimensional electron gases (2DEGs) proposed for spin manipulation are mainly based on the spin–orbit (SO) interaction. The SO Hamiltonian reads [8]

$$\hat{H}_{\mathrm{SO}} = -\frac{\lambda_0^2}{\hbar} e\mathbf{E}(\mathbf{r})[\hat{\sigma} \times \hat{\mathbf{p}}]. \tag{1}$$

Here $\mathbf{E}(\mathbf{r})$ is the electric field, $\hat{\sigma}$ are the Pauli matrices, $\hat{\mathbf{p}}$ is the canonical momentum operator, $\mathbf{r}$ is a 3D position vector, $\lambda_0^2 = \hbar^2/(2m_0c)^2$ and m_0 is the electron mass in a vacuum. In materials m_0 and λ_0 are substituted by their effective values m^* and λ. A significant SO term arises from

the interaction of the travelling charge carrier with strong electric fields in solids. The SO term can be seen as the interaction of the electron spin with the magnetic field, B_{eff}, appearing in the rest frame of the electron.

2. Rashba coupling

In the case of quantum heterostructures of narrow gap semiconductors, a major contribution to the SO coupling may originate intrinsically from its confining potential [9]. The spin Hall effect in two-dimensional (2D) electron systems exploits the Rashba SO coupling (α-coupling) due to an asymmetry in the quantum well potential that confines the electron gas [10]. The main component of the SO coupling will be along $\hat{z}$, and the Hamiltonian in equation (1) will take the form [11] $\hat{H}^{\alpha}_{\text{SO}} = \frac{\alpha}{\hbar}[\sigma_{\mathbf{x}}\mathbf{p}_{\mathbf{y}} - \sigma_{\mathbf{y}}\mathbf{p}_{\mathbf{x}}]$. α in a vacuum is $\lambda_0^2 E_z e$ while the highest value of α in 2DEGs is close to to 10^{-10} eV m as reported in [12, 13].

The α-SO coupling may generate a spin-dependent transverse force on moving electrons [14–17]. This force tends to separate different spins in the transverse direction as a response to the longitudinal charge current, giving a qualitative explanation for the Rashba spin Hall effect. In the presence of Rashba SO coupling, however, the electron spin, particularly its out-of-plane projection, is not conserved, and hence the usual continuity equation fails to describe the spin transport. This makes the spin transport phenomena in this system rather complicated.

3. Lateral-confinement-induced coupling

Next we consider low-dimensional electron systems formed by crossing quantum wires (QWs) through the analysis of the SO coupling in a 2D electron system with an in-plane potential gradient. In such systems a confining (β-coupling) SO term arises from the in-plane electric potential that is applied to squeeze the 2DEG into a quasi-one-dimensional channel [10, 18].

We adapt the general form of equation (1) to the strictly 2D case, where the degree of freedom of motion in the z direction is frozen out ($\langle p_z \rangle = 0$), and the potential energy, V_{c}, depends only on x and y coordinates. Then the SO Hamiltonian in this case can be written in the form [19]:

$$\hat{H}^{\beta}_{\text{SO}} = \frac{\lambda^2}{\hbar}\hat{\sigma_z}[\nabla V_{\text{c}}(x, y) \times \hat{\mathbf{p}}]_z. \tag{2}$$

The reduced Hamiltonian commutes with the spin operator $S_z = \hbar/2\sigma_z$, and hence conserves spin. Thus SO coupling of this kind generates a spin-dependent force on moving electrons while conserving their spins. The standard continuity equation for spin density and spin current is naturally established because of spin conservation.

The spin-conserving β-SO interactions are also at the basis of the quantum spin Hall effects discovered recently [20–24].

4. Spin filters

In this paper we investigate the spin polarization of the current in the presence of (spin conserving) β-interaction in a T-shaped conductor; in particular we show why a β-coupling scheme results in a different working principle, as compared to equivalent structures exploiting α-coupling [25].

In fact *'spin filters'* based on α-coupling rely on the precession of electrons spins during their motion through the wave guides, while the scheme we propose here, based on β-coupling,

preserves the $\hat{z}$ component of the spin at the injection and sends electrons/holes to different stubs according to their spin value. Differently from α-coupling schemes, the device we propose should in principle allow one, for a given charge current, to electrically measure the spin polarization grade with its sign. As a first step in support of this statement we write down the Hamiltonian of a T-stub with SO β-coupling and make some qualitative considerations. In the following step we extract a quantitative analysis of a device's transport properties using materials parameters from the literature.

4.1. β-SO coupling and effective magnetic field

Here we focus on the case of pure β-coupling.

The basic building blocks of the nanojunctions that we discuss in the following are the QWs. The ballistic one-dimensional wire is a nanometric solid-state device in which the transverse motion (along ξ) is quantized into discrete modes, and the longitudinal motion (in the η direction) is free. In this case electrons are envisioned to propagate freely down a clean narrow pipe and electronic transport with no scattering can occur.

In a quasi one-dimensional wire, where a parabolic lateral confining potential [26] along ξ ($\xi \equiv x$ for leads 1 and $\xi \equiv y$ for leads 2 and 4) with force ω_d is considered ($V(\mathbf{r}) \equiv V(\xi) = \frac{m^*\omega_d^2}{2}\xi^2$) it follows

$$\hat{H}_{\mathrm{SO}}^{\beta} = \frac{\beta}{\hbar}\frac{\xi}{l_\omega}(\hat{\sigma} \times \hat{\mathbf{p}})_\xi \simeq \mathrm{i}\beta\frac{x}{l_\omega}\sigma_z\frac{\partial}{\partial\eta}, \tag{3}$$

where $l_\omega = (\hbar/m^*\omega_d)^{1/2}$ is the typical spatial scale and η is the other direction in the 2DEG ($\eta \perp \xi$). Thus, as we discussed in a previous paper [20], in a QW a uniform *effective magnetic field*, B_{eff}, is present along z:

$$\widetilde{B}_{\mathrm{eff}} = \frac{\lambda^2}{\hbar}m^{*2}\omega_d^2 c \equiv \frac{\beta}{\hbar l_\omega}\frac{m^* c}{e}. \tag{4}$$

Then an electron of spin $S_z = s\hbar/2$ flowing in the QW perceives in its rest frame a magnetic field B_{eff} directed upward or downward according to the sign of s. This results in an interesting behaviour of junctions between two wires, such as T stubs and cross junctions, when a large enough β-coupling is considered.

The discussion reported above for a QW can be generalized to any device patterned in a 2DEG. The Hamiltonian of an electron moving in a 2D device defined by a general confining potential $V_{\mathrm{c}}(r)$ in which the α-SO term is negligible can be written as

$$H = \frac{\mathbf{p}^2}{2m^*} + \frac{\lambda^2}{\hbar}e(\mathbf{E}(\mathbf{r}) \times \mathbf{p})_z\sigma_z + V_{\mathrm{c}}(\mathbf{r}) = \frac{\pi^2}{2} + V_{\mathrm{c}}(\mathbf{r}) - \frac{\lambda^4 m^*}{2\hbar^2}e^2|\mathbf{E}(\mathbf{r})|^2, \tag{5}$$

where $\pi_i = (p_i - \epsilon_{ijz}\frac{\lambda^2}{\hbar}m^* e E_j\sigma_z)$ and $\mathbf{E}(\mathbf{r}) = \boldsymbol{\nabla} V_{\mathrm{c}}(\mathbf{r})$.

The commutation relation

$$[\pi_x, \pi_y] = -\mathrm{i}\hbar\left(\frac{\lambda^2}{\hbar}m^* e\nabla\cdot\mathbf{E}\right)\sigma_z \equiv -\mathrm{i}\hbar\frac{e}{c}B_{\mathrm{eff}}(\mathbf{r})\sigma_z$$

is equivalent to that of a charged particle in a transverse magnetic field, but here the sign of $B_{\mathrm{eff}}(\mathbf{r})$ depends on the direction of the spin along $\hat{z}$. It follows that electrons with opposite spin states are deflected into opposite terminals by a spin-dependent Lorentz force:

$$\mathbf{F} = m^*\ddot{\mathbf{r}}(t) = -\nabla V_{\mathrm{c}}(\mathbf{r}) + \frac{e}{m^* c}(\mathbf{B}(\mathbf{r}) \times \pi), \tag{6}$$

where $\mathbf{B}(\mathbf{r}) \equiv s B_{\mathrm{eff}}(\mathbf{r})\hat{z}$ is a spin-dependent inhomogeneous magnetic field, with $s = \pm 1$.

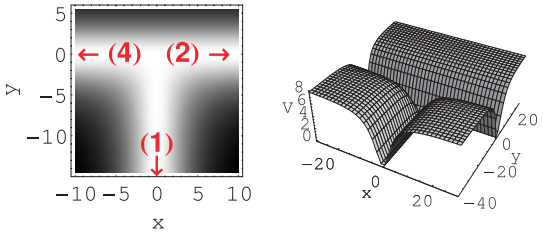

Figure 1. Density and 3D plots of the potential $V_c(x, y)$ which models a T-shaped conductor. This device can be assumed as a crossing junction between two quasi one-dimensional wires of width W which ranges from ∼25 up to 100 nm.

4.2. The T junction

In a cross junction sample, the confining electrostatic potential for an electron is not exactly known. However, it is plausible that there has to be a potential minimum at the centre of the junction. In this respect, it would be appropriate to qualitatively model the smooth confining potential, displayed in figure 1, of a T-stub structure as

$$V_T(x, y) = \frac{m^*}{2}\omega_d^2 R^2 \frac{x^2 y^2}{(R^2 + x^2)(R^2 + y^2)}\vartheta(-y) + \frac{m^*}{2}\omega_d^2 R^2 \frac{y^2}{(R^2 + y^2)}\vartheta(y), \tag{7}$$

where $\vartheta(y)$ is a regular function which approximates the step function ($\vartheta(y) \sim (1 + \tanh(y/\rho))/2$ with $\rho \ll l_\omega$). Here R represents the effective radius of the crossing zone, while l_ω can be related to the effective width of the wires W, which is known to be smaller than the lithographically defined one and can be further reduced by using etched side gate electrodes. This technique also works on small gap semiconductors such as InGaAs [27] featuring a small Schottky barrier with metals. In general, one can relate the frequency ω_d to W as $\omega_d \sim \frac{(2\pi)^2}{2}\frac{\hbar}{m^* W^2}$. This expression can be obtained by comparing the energy levels of a harmonic oscillator to those of a square potential well.

Far from the crossing zone, the confining potential describing the wires reads as $V_c(x, -\infty) \sim \frac{m^*}{2}\omega_d^2 x^2$ or $V_c(\pm\infty, y) \sim \frac{m^*}{2}\omega_d^2 y^2$. Thus, asymptotically B_{eff} is given by equation (4). To have an idea of the strength of this magnetic field, we compare the cyclotron frequency $\omega_c = e\widetilde{B}_{\text{eff}}/(m^* c)$ with ω_d:

$$\widetilde{B}_{\text{eff}} \sim \frac{(2\pi)^4}{4}\frac{\hbar c}{e}\frac{\lambda^2}{W^4} \leftrightarrow \frac{\omega_c}{\omega_d} \sim \frac{(2\pi)^2}{2}\frac{\lambda^2}{W^2}. \tag{8}$$

We report all our results as a function of the ratio ω_c/ω_d. In numerical calculation ω_c/ω_d takes values that are in the range defined by experiments on 2DEGs. We estimate the effective value of λ in the 2DEG from the measured value of α in the literature [12, 28] and from the calculated band diagram of the same structures. In InGaAs/InP heterostructures λ^2 takes values between 0.5 and 1.5 nm^2. For GaAs heterostructures λ^2 is one order of magnitude less than in InGaAs/InP, whereas for HgTe based heterostructures it can be more than three times larger [13, 28]. Since the lithographical width of a wire defined in a 2DEG can be as small as 20 nm [29], we assume that ω_c/ω_d runs from 1×10^{-6} to 1×10^{-1}. In any case W should be larger than λ_F, so that at least one conduction mode is occupied.

4.3. Ballistic transport and calculations

Here we report a numerical study, limited to a single channel transport, i.e. we assume that just the lowest subband of the QW is activated. When the characteristic sizes of semiconductor

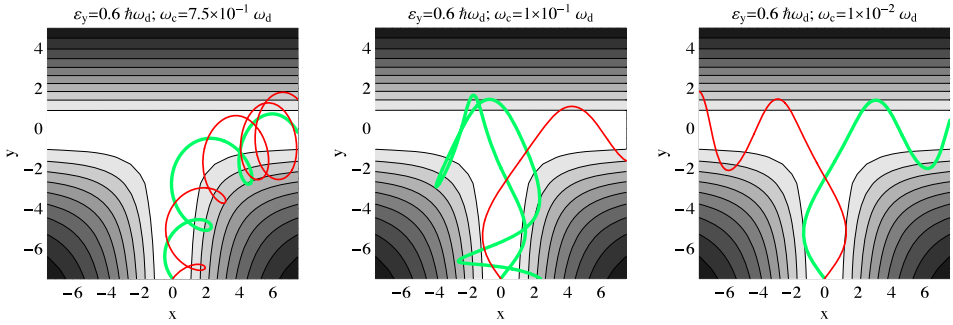

Figure 2. Trajectories of the charges in the T junction without SO. Each panel is for a different value of the external magnetic field. Red and green curves correspond to trajectories of the electrons injected in lead 1 with the same energy and opposite v_x.

devices are smaller than the elastic mean free path of charge carriers, the carrier transport becomes ballistic. It follows that the transport can be studied starting from the probability of transmission from a probe to another one following the Büttiker–Landauer formalism [30].

The calculation of the transmission amplitude is based on the simulation of classical trajectories of a large number of electrons with different initial conditions. We want to determine the probability $T_{1j}^{s,s'}$ of an electron with spin s to be transmitted to lead j with spin s' when it is injected in lead 1. This coefficient can be determined from classical dynamics of electrons injected at $y_0 = -7.5l_\omega$ (emitter position) with an injection probability following a spatial distribution $p_0(x_0, y_0) \propto \mathrm{e}^{-\frac{x_0^2}{l_\omega^2}}$ as in [31]. The total energy ε of a single electron is composed of the free electron energy ε_y^0 for motion along y and the energy of the transverse mode considered ε_x^0 due to the parabolic confinement ($\varepsilon_x = \hbar\omega_d/2$ for the lowest channel).

Thus, we have calculated $T_{ij}^{s,s'}$ determined by numerical simulations of the classical trajectories injected into the junction potential V_c with boundary conditions [24] $\mathbf{r}(0) \equiv (x_0, y_0)$; $\mathbf{v}(0) \equiv \mathbf{v}_0$, each one with a weight $p_0(x_0)$. In general these transmission amplitudes can depend on the position of the collectors along the probes. In this paper we take into account $N_t = 804$ classical trajectories for each value of the parameters.

Before the discussion about our results we want to point out that a comparison involving theoretical and experimental results allowed us to test our approach. In fact in [24] we investigated the effects on the X-junction transport due to a quite small external magnetic field, B_{ext}, by focusing on the so-called *quenched region*. The measured 'quenching of the Hall effect' [32] is a suppression of the Hall resistance or 'a negative Hall resistance' R_{H} for small values of B_{ext}. The results reported in [24] showed a good agreement with the experimental data, thus confirming the reliability of our approach.

In order to show how the symmetry breaking produces a transverse current I_{H}, we briefly discuss the case of a T-shaped junction, without a SO term, in a uniform external magnetic field B directed along $\hat{z}$: in figure 2 we report the corresponding classical electron trajectories. The increase of the magnetic field results in a broken symmetry between leads 2 and 4 and makes the probabilities of transmission in the two leads very different.

The current I_i at lead i of a multi-probe device can be expressed in terms of chemical potentials $\mu_j = eV_j$ at each lead and of the transmission coefficient T_{ij} as $I_i = e^2/h \sum_j T_{ij}(V_i - V_j)$; normalization requires $\sum_j T_{ij} = 1$ [30, 31]. Thus to an injected current I_0 in lead 1, it corresponds a transverse Hall current

$$I_{\mathrm{H}} = (T_{12} - T_{14})I_0.$$

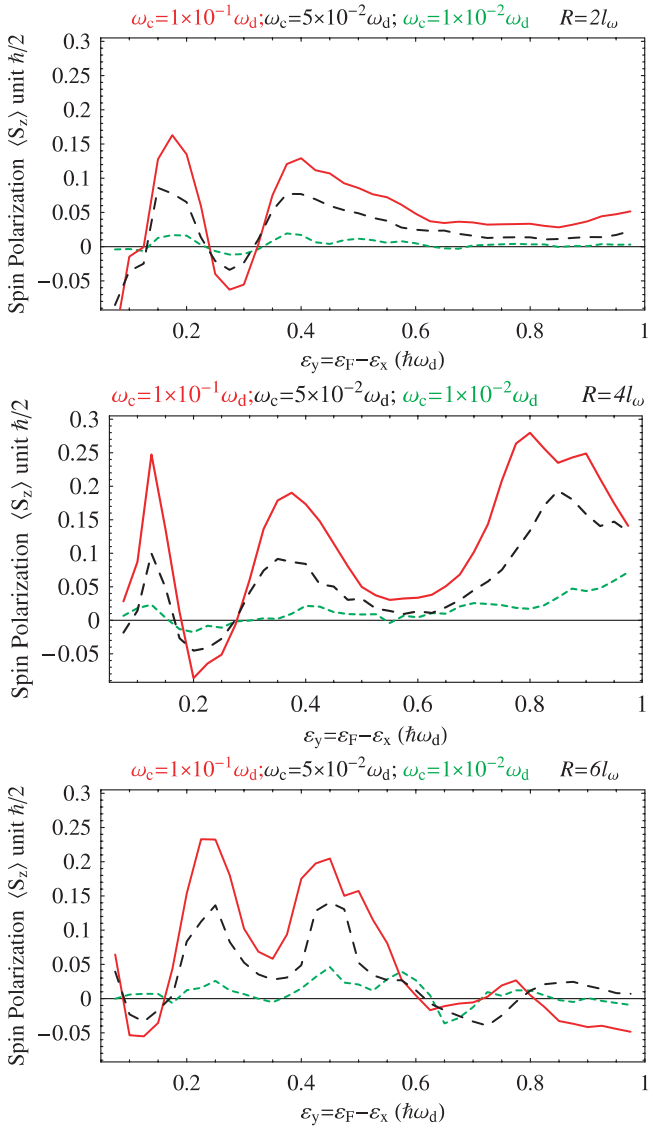

Figure 3. Spin polarization at lead 2 $\langle S_z \rangle$ as a function of the Fermi energy ε_F in the case of zero external magnetic field and β-SO coupling for three different values of the radius R of the crossing zone. Around $\varepsilon_y = 0.2\hbar\omega_d$ (or, to be precise, in the range of values 0.1–0.3 depending on the value of R) there is a quenching region corresponding to an inversion of the spin polarization [24].

This Hall current is mainly due to the electric field $\nabla V_c(\mathbf{r})$ for $y > 0$ and to the broken symmetry between leads 4 and 2 due to the magnetic field.

5. Spin–orbit and effective magnetic field

In figure 3 we report the spin polarization of the transverse current, when considering a vanishing external magnetic field and a β-coupling SO term. Numerical calculations are performed using the procedure discussed above. Thus, we show the spin polarization $\langle S_z \rangle$

of the current flowing along the x direction. $\langle S_z\rangle$ corresponds to

$$\langle S_z\rangle = \frac{\hbar}{2}\frac{T_{21}^{\uparrow\uparrow} - T_{21}^{\downarrow\downarrow}}{T_{21}^{\uparrow\uparrow} + T_{21}^{\downarrow\downarrow}} \equiv \frac{\hbar}{2}P_z,$$

in this special case where $T_{ij}^{\uparrow\downarrow} = T_{ij}^{\downarrow\uparrow} = 0$, because of the commutation between $\hat{S}_z$ and $\hat{H}_{\mathrm{SO}}^{\beta}$ and $T_{12}^{\uparrow\uparrow} = T_{14}^{\downarrow\downarrow}$, $T_{14}^{\uparrow\uparrow} = T_{12}^{\downarrow\downarrow}$ since the effective magnetic field depends on the spin orientation of electrons injected in 1.

Starting from the number of trajectories we are able to estimate the statistical fluctuation on the calculated $\langle S_z\rangle$,

$$\sigma_{S_z} \lesssim \frac{\hbar}{2}\frac{\sigma_B}{N_t} \sim \frac{\hbar}{2}0.018,$$

where we take $\sigma_B \propto \sqrt{N_t}$ according to the binomial distribution.

Notice that for ε_y between 0.1 and $0.3\hbar\omega_d$ there is an inversion of the spin polarization ($\langle S_z\rangle < 0$) for each panel of figure 3. It is well known that a strong geometric dependence of the transport properties was shown in the presence of a transverse magnetic field by giving a negative Hall current, as we discussed above concerning the 'quenching of the Hall effect'. In fact, the resistances measured in narrow-channel geometries are mainly determined by the scattering processes at the junctions with the side probes which depend strongly on the junction shape [33]. This dependence of the low-field Hall current was demonstrated in [34] and measured in [32]. In a recent paper [24] it was discussed how the effective field generated by the β-SO coupling characterizes a regime of transport that can be assumed as the *quenching regime of the SHE*. Hence, it follows that the inversion of the spin polarization, shown in figure 3, can be explained on the same grounds. Moreover, this behaviour has a clear signature around $\varepsilon_y \sim 0.1 - 0.3\hbar\omega_d$, while for other values of the Fermi energy the calculated quenching is comparable with the statistical fluctuation due to the numerical approach.

The geometric dependence of $\langle S_z\rangle$ can be clearly inferred by comparing the three panels of figure 3, where we show the effects of the width of the crossing region (R). We can conclude that a significant spin polarization of the transverse current can be obtained at some fixed values of the Fermi energy, and that a more efficient process is given by the junction with $R \sim 4l_\omega$, while $\langle S_z\rangle$ can be attenuated in larger or smaller junctions.

By comparing figures 2 and 4, where some trajectories are shown, we can understand the microscopic mechanism which produces the transverse spin current by focusing on the symmetry breaking between the spin-up and spin-down electrons.

In order to evaluate the order of magnitude corresponding to the spin polarization, we can calculate the dependence of $\langle S_z\rangle$ on the strength of the β-SO coupling. In figure 5 we show the value of the spin polarization, as it can be measured at lead 2, for different strengths of β-coupling ranging over five orders of magnitude.

We distinguish two cases according to the possibilities that in lead 1 is injected, respectively: (i) a non-polarized current or (ii) a polarized charge current. In case (i), there is no charge current between leads 2 and 4, but a pure spin current, I_{SH}, that is proportional to $T_{12}^{\uparrow\uparrow} - T_{12}^{\downarrow\downarrow}$. This quantity can also be read as the spin polarization $\langle S_z\rangle$ of the current in lead 2, when an unpolarized spin current is injected in lead 1. Figure 3 shows that, for some energies, this spin current quenches and eventually reverses its sign. The same is observed for a fixed value of the energy, when changing the parameter ω_c (different values of ω_c could be experimentally obtained by changing the value of the effective width of the wires defining the T junction, or by changing the value of the coupling parameter). This phenomenon has been treated in a recent paper [24] studying the transport through micrometric ballistic 4-probe X-junctions, where it was found that this magneto-transport anomaly is closely related to the

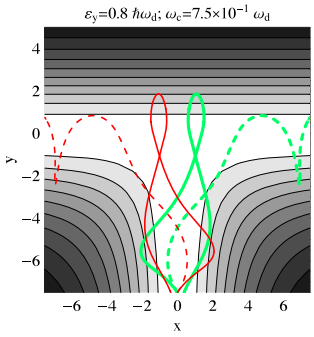

Figure 4. Trajectory of an electron in a T junction ($R = 4l_\omega$) with the β-SO term and vanishing external magnetic field. Electrons are injected in lead 1 with a defined spin orientation along $\hat{z}$. Dashed lines correspond to $e^{\downarrow}$ and solid lines to $e^{\uparrow}$. Electrons are injected with the same energy and opposite $\pm v_x$, (+red, −green).

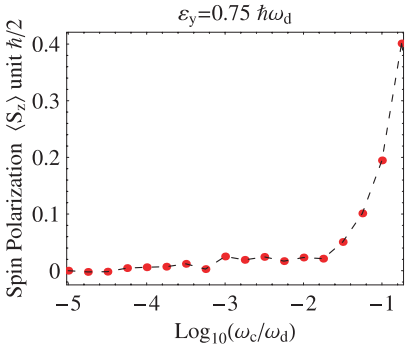

Figure 5. Spin polarization at lead 2 $\langle S_z \rangle$ as a function of the β coupling strength (given by $\log_{10}(\omega_c/\omega_d)$), for a fixed value of the Fermi energy $\varepsilon_F \sim 0.75\hbar\omega_d$, in the case of vanishing external magnetic field and β-SO coupling ($R = 4l_\omega$).

quenched or negative Hall resistance. In case (ii) a charge current flows between leads 2 and 4, as can be seen considering a completely polarized injected current (e.g. having all electrons with spin up). In that case $T_{12}^{\uparrow\uparrow} - T_{14}^{\uparrow\uparrow}$ will be proportional to a charge current flowing between leads 2 and 4. It is easy to see that, even if the current is not completely polarized, there will be a charge current flowing between leads 2 and 4 that is proportional to the polarization degree of the injected current,

$$I_{24} \propto G_{24} = \frac{e^2}{h} \epsilon P_z^0,$$

where G_{24} is the charge conductance, $\epsilon \equiv T_{12}^{\uparrow\uparrow} - T_{12}^{\downarrow\downarrow}$ and P_z^0 is the spin polarization of the injected current. This scheme would implement the electric detection of a spin polarized current.

6. Conclusion

We described a system based on SO β-coupling capable of spin filtering and electric based spin polarization measurements. The results we have shown were obtained using values of λ and W well within those given by currently available 2DEGs and nanolithography techniques. The

use of a series of T nanojunctions could also give some better results in the spin polarization of the emerging current.

The proposed devices also represent a new test for the effects of the β-SO interactions which are at the basis of the quantum spin Hall effects recently discussed in several papers [20–24]. In these papers the α-coupling was always assumed to be negligible, although in general this term is comparable to (or larger than) the β one. However, it can be shown that spin polarization effects of the β-coupling should be some orders of magnitude larger than the those calculated for α coupling of a comparable strength [24].

References

[1] Awschalom D D, Loss D and Samarth N 2002 *Semiconductor Spintronics and Quantum Computation* (Berlin: Springer)
Kane B E *et al* 1998 *Nature* **393** 133
[2] D'yakonov M I and Perel' V I 1971 *JETP Lett.* **13** 467
[3] Sinova J, Culcer D, Niu Q, Sinitsyn N A, Jungwirth T and MacDonald A H 2004 *Phys. Rev. Lett.* **92** 126603
[4] Hirsch J E 1999 *Phys. Rev. Lett.* **83** 1834
[5] Hankiewicz E M, Molenkamp L W, Jungwirth T and Sinova J 2004 *Phys. Rev.* B **70** 241301
[6] Kane C L and Mele E J 2005 *Phys. Rev. Lett.* **95** 226801
[7] Sheng L, Sheng D N, Ting C S and Haldane F D M 2005 *Phys. Rev. Lett.* **95** 136602
[8] Landau L D and Lifshitz E M 1991 *Quantum Mechanics* (Oxford: Pergamon)
[9] Bychkov Yu A and Rashba E I 1984 *Pis. Zh. Eksp. Teor. Fiz.* **39** 66
Bychkov Yu A and Rashba E I 1984 *JETP Lett.* **39** 78 (Engl. Transl.)
[10] Kelly M J 1995 *Low-dimensional Semiconductors: Material, Physics, Technology, Devices* (Oxford: Oxford University Press)
[11] Bellucci S and Onorato P 2005 *Phys. Rev.* B **72** 045345
Bellucci S and Onorato P 2003 *Phys. Rev.* B **68** 245322
[12] Engels G, Lange J, Schäpers Th and Lüth H 1997 *Phys. Rev.* B **55** R1958
[13] Schultz M, Heinrichs F, Merkt U, Colin T, Skauli T and Løvold S 1996 *Semicond. Sci. Technol.* **11** 1168
[14] Shen S-Q 2005 *Phys. Rev. Lett.* **95** 187203
[15] Nikolic B K, Zarbo L P and Welack S 2005 *Phys. Rev.* B **72** 075335
[16] Zhou B, Ren L and Shen S-Q 2006 *Phys. Rev.* B **73** 165303
[17] Berard A and Mohrbach H 2006 *Phys. Lett.* A **352** 190
[18] Thornton T J, Pepper M, Ahmed H, Andrews D and Davies G J 1986 *Phys. Rev. Lett.* **56** 1198
[19] Moroz A V and Barnes C H W 2000 *Phys. Rev.* B **61** R2464
[20] Bellucci S and Onorato P 2006 *Phys. Rev.* B **73** 045329
[21] Bernevig B A and Zhang S-C 2006 *Phys. Rev. Lett.* **96** 106802
[22] Jiang Y and Hu L 2006 *Preprint* cond-mat/0603755
[23] Hattori K and Okamoto H 2006 *Phys. Rev.* B **74** 155321
[24] Bellucci S and Onorato P 2006 *Phys. Rev.* B **74** 245314
Bellucci S and Onorato P 2007 *Phys. Rev.* B **75** 235326
[25] Kiselev A A and Kim K W 2001 *Appl. Phys. Lett.* **78** 775
[26] Laux S E, Frank D J and Stern F 1988 *Surf. Sci.* **196** 101
Drexler H *et al* 1994 *Phys. Rev.* B **49** 14074
Kardynał B *et al* 1997 *Phys. Rev.* B **55** R1966
[27] Carillo F, Biasiol G, Frustaglia D, Giazzotto F, Sorba L and Beltram F 2006 *Physica* E **32** 53
[28] Zhang X C, Pfeuffer-Jeschke A, Ortner K, Hock V, Buhmann H, Becker C R and Landwehr G 2001 *Phys. Rev.* B **63** 245305
[29] Knop M, Richter M, Maßmann R, Wieser U, Kunze U, Reuter D, Riedesel C and Wieck A D 2005 *Semicond. Sci. Technol.* **20** 814
[30] Büttiker M 1986 *Phys. Rev. Lett.* **57** 1761
[31] Geisel T, Ketzmerick R and Schedletzky O 1992 *Phys. Rev. Lett.* **69** 1680
[32] Ford C J B, Washburn S, Büttiker M, Knoedler C M and Hong J M 1989 *Phys. Rev. Lett.* **62** 2724
[33] Timp G, Baranger H U, deVegvar P, Cunningham J E, Howard R E, Behringer R and Mankiewich P M 1988 *Phys. Rev. Lett.* **60** 2081
[34] Baranger H U and Stone A D 1989 *Phys. Rev. Lett.* **63** 414